Optical Detection Method for Partial Discharge of Printed Circuit Boards in Electrified Aircraft under Various Pressures and Voltages

Zang, Yiming ; Ghaffarian Niasar, Mohamad; Qian, Yong; Zhou, Xiaoli; Sheng, Gehao; Jiang, Xiuchen; Vaessen, Peter

DOI
10.1109/TTE.2022.3191308

Publication date
2022

Document Version
Accepted author manuscript

Published in
IEEE Transactions on Transportation Electrification

Optical Detection Method for Partial Discharge of Printed Circuit Boards in Electrified Aircraft under Various Pressures and Voltages

Yiming Zang, Mohamad Ghaffarian Niasar, Yong Qian, Xiaoli Zhou, Gehao Sheng, *Member*, *IEEE*, Xiuchen Jiang and Peter Vaessen, *Member, IEEE*

***Abstract*—Realization of an electrical aircraft demands a low weight electric distribution and propulsion system. The use of high voltage and power electronics operated at high switching frequencies is essential to achieve this objective. However, printed circuit boards (PCBs) in electrified aircraft are in a harsh working environment, which can make PCBs more susceptible to generate partial discharges (PD). The current PD detection technology has poor immunity to the electromagnetic interference and acoustic interference in the operating environment of aircraft. Therefore, this paper proposes an optical-based PD detection method for PCBs, which is effectively immune to electromagnetic and acoustic interference. This method uses fluorescent fiber as a PD optical signal sensor, and then collects the optical signal by the avalanche photodiode (APD). Experiments have verified that the detection sensitivity, sensing range and anti-interference performance of this method are well satisfied with the PD detection. In addition, single PD pulse, optical phase resolved PD patterns and PD inception voltage under different air pressure and voltage conditions are investigated. Finally, the relationship between the optical signal and PD amplitude is found to be proportional, which proves that the severity of the PD on PCBs can be effectively detected and evaluated by this method.**

***Index Terms*—partial discharge, printed circuit boards, optical detection, electrified aircraft, fluorescent fiber.**

This work was supported in part by the National Natural Science Foundation of China under Grant No. 62075045.

Yiming Zang, Yong Qian, Gehao Sheng and Xiuchen Jiang are with the Department of Electrical Engineering, Shanghai Jiao Tong University, Shanghai 200240, China (e-mail: zangyiming@sjtu.edu.cn; qian_yong@sjtu.edu.cn; shenghe@sjtu.edu.cn; xcjiang@sjtu.edu.cn).

Mohamad Ghaffarian Niasar (*corresponding author*), and Peter Vaessen are with the Delft University of Technology, Mekelweg 4, 2628 CD, Delft, Netherlands (e-mail: M.GhaffarianNiasar@tudelft.nl; P.T.M.Vaessen@tudelft.nl).

Xiaoli Zhou is with the Department of Light Sources and Illuminating Engineering, School of Information Science and Technology, Fudan University, Shanghai 200433, China (e-mail: zhouxl@fudan.edu.cn).

I. Introduction

As the demand for safety, eco-friendliness and efficiency of aircraft increases, more/all-electric aircraft (MEA/AEA) has been widely used in recent years [1]. For MEA/AEA, efficient electrical drives require a high-power density, which means that a large number of printed circuit boards (PCBs) are required to enable the operation of the electrical system in the avionics [2]. Although the higher voltage amplitude and voltage frequency variation can help increase the power density, yet this also brings a greater threat to the electrical insulation of PCBs [3]. Since some components in the electric aircraft operate under the high-frequency electrical stress, in a low-pressure environment, and due to compacting electronic circuitry to reduce space and weight in aircraft, all together it makes the insulation performance more critical compared to that of conventional electrical equipment on land [4, 5]. Therefore, there is an urgent need to assess the insulation status of PCBs in aircraft, to avoid irreversible and serious failures. In addition, PCBs for aircraft need insulation testing for quality control before they are put into service, and such a harsh environment also needs to be simulated during testing.

Partial discharge (PD) is a precursor and a major cause of insulation degradation, which is mainly detected by collecting the acoustic, optical and electrical signals generated by the PD source [6]. By detecting PD occurring on PCBs, the insulation status can be evaluated so that PCBs can be maintained before breakdown, effectively ensuring the safety of aircraft.

At present, there are a number of studies on the PD detection in MEA/AEA, of which the PD detection on PCBs is relatively lacking. Several methods based on the detection of pulse currents and ultra-high frequency (UHF) signals are used to detect PDs for aircraft motors [7-9]. These methods can be applied for 50/60Hz voltage, but are susceptible to electromagnetic interference in the environment of high-frequency square voltages. Methods based on the detection of acoustic vibration signals generated by PD sources are also proposed for PD detection by using a Sagnac optical fiber and Fabry-Perot optical fiber, however, there is a large amount of mechanical vibration interference of the equipment during the operation of the aircraft which reduces the detection performance [10, 11]. In order to reduce electromagnetic and acoustic interference during PD detection, PD detection by detecting PD radiation photons has been proposed. There are detecting the PD occurrence in power equipment by fluorescent optical fibers, classical photomultiplier tubes and silicon photomultiplier, and also using spectroscopy to study the optical PD behavior [12]. However, there are few related studies that introduce fluorescent optical fibers into MEA/AEA for PD detection of PCBs.

Regarding PDs on PCBs, there are several studies about the breakdown characteristics and PD testing of PCBs under AC 50Hz voltage, but there are few investigations of the PD characteristics on PCBs under AC voltage for other frequencies and square voltages, which are prevalent in real MEA/AEA power system [13-15]. Some work about the effect of conformal coating and the influence of external environmental changes on PCB partial discharges is done [16, 17]. However, these studies mainly focus on the electrical and

physicochemical properties of the PCB itself, which cannot be applied to detect and forewarn about the PDs in MEA/AEA. In addition, the optical PD behavior of PCBs in MEA/AEA is also an important factor that can reflect the insulation state, which is essential to be studied to detect the health status of PCBs.

Therefore, this paper proposes a novel method for detecting PDs on PCBs based on the fluorescent fiber. In order to adapt to the actual operating conditions in MEA/AEA, PD phenomena of PCBs at low air pressure and different voltages (sinusoidal and square voltages of different frequencies) are investigated. The research in this paper not only proposes an anti-electromagnetic and anti-acoustic interference optical PD detection method in MEA/AEA, but also fills the gap in the optical PD characteristics of the PCB under different operation conditions. Since the PD performance testing before the PCBs are used into aircraft has the same interference as the actual operating conditions in MEA/AEA, this method also provides a new PD detection method on PCB testing for pre-qualification control.

The paper is organized as follows, Section II gives detailed information for optical detection methods of PDs on PCBs. The design of PCB samples, the construction of the PD experimental platform and the main experimental contents are described in Section III. Section IV verifies the effectiveness of the optical method in terms of both anti-interference performance and detection distance. The pulse and phase resolved partial discharge (PRPD) patterns and PD inception voltage (PDIV) of PCBs are described in Section V. The relationship between the optical signal and the PD severity is investigated in Section VI and Section VII gives the conclusion.

II. Optical PD Detection Method Based on Fluorescent Fibers

A. Principle of the fluorescent fiber

Fluorescent fiber is a kind of special fiber that absorbs incident light with a certain wavelength range through some fluorescent substances in the core of the fiber and then the fluorescent substances excited and emit fluorescence. When fluorescent substances are activated by the absorption of a light signal, the electrons of the fluorescent molecule transition from the ground state to the excited state. The electrons are unstable in the excited state and will return to the ground state, the process of which releases photons (fluorescence) that propagate through the fiber, thus detecting the light signal. In this process, the fluorescent substances will be excited to radiate light with a different wavelength from the incident light, which is called Stokes Shift. This shift value of the wavelength is typically 100~200nm.

The advantage of fluorescent fiber over traditional quartz fiber is that its sensing is not limited by the numerical aperture angle, and the fluorescent material in it can receive light from all directions through the transparent cladding [18]. In contrast, conventional quartz fibers are limited by the numerical aperture angle and can only detect light from a limited direction. Since the light of PDs on PCBs can come from any direction, in this paper we propose to use fluorescent fibers to sense the light signals generated by the PD source, which can receive more light signals and be well adapted to the detection environment of PCBs. The schematic diagram of optical sensing for the fluorescent fiber is shown in Fig. 1.

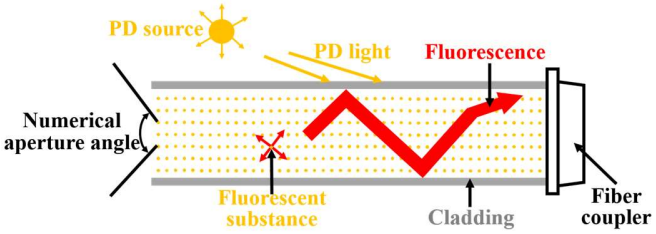

Fig. 1. Schematic diagram of fluorescent fiber optical signal sensing principle.

When the light generated by the PD is incident into the fluorescent fiber, the optical radiation generated by the excitation of the fluorescent substances satisfies the total reflection condition of the core-cladding interface [19]. All the excited fluorescence will be transmitted axially along the fiber, which has high detection efficiency. Regarding transmission loss, the increase in length of conventional quartz fibers can increase transmission loss. However, since the fluorescent fiber can receive light signal at everywhere along the fiber itself, the increase of fluorescent fiber length is equivalent to increase the receiving area of light signal, which can simultaneously enhance the signal strength. Moreover, considering that the PCB packaging in MEA/AEA are generally small (< 1m), the overall loss from the length is very small. The material of the fluorescent fiber is polymethyl methacrylate (average dielectric constant is around 3.36 and average dielectric strength is 25.3 kV/mm), which has good insulation performance, high optical transmission efficiency, strong toughness and stable chemical properties, which are well suited for the harsh working environment in aircraft [18].

B. Optical sensing of PD

In order to convert the optical signal collected by the fluorescent fiber into a more easily analyzed electrical signal, in this paper an avalanche photodiode (APD) for photoelectric signal conversion is used. APD is an optical sensor with high sensitivity. Currently, a photomultiplier tube (PMT) is more used in the laboratory for photoelectric signal conversion, which has the disadvantage that it is large and need high power supply. However, APD is not only small in size, but also has good immunity to magnetic interference [20], which is more suitable for aircraft applications.

Considering the Stokes Shift and optical signal acquisition, not only the excitation spectrum of the fluorescent fiber to the PD emission spectrum needs to be met, also the radiation spectrum of the fluorescent fiber to the response spectrum of the APD has to be met. Although the above spectral matching relationships do not need to be an exact match, the major wavelengths need to be satisfied. PDs on PCBs occur mostly between copper conductors, and their discharge emission spectra are predominantly distributed between 300~650nm [21]. The effective response spectrum range of the APD (Type: APD130A2) selected in this paper is mainly between 350-850 nm. Therefore, according to these spectral relationships, a fluorescent fiber doped with Alexa Fluor 546 fluorescent substance is selected as the optical sensor in this paper. The specific distribution of the four spectra are shown in Fig. 2.

Since the units of the various spectral response intensities are different, the units in Fig. 2 are normalized. The relationship between the main ranges of the spectrum can also be illustrated by the relative spectral response intensities. It can be seen that the matching relationship between the four spectra essentially satisfies the sensing conditions. The excitation spectrum of the fiber overlaps significantly with the main bands of the spectra of PD emission. Moreover, the emission spectrum of optical fiber is highly coincident with the band of high response efficiency of APD.

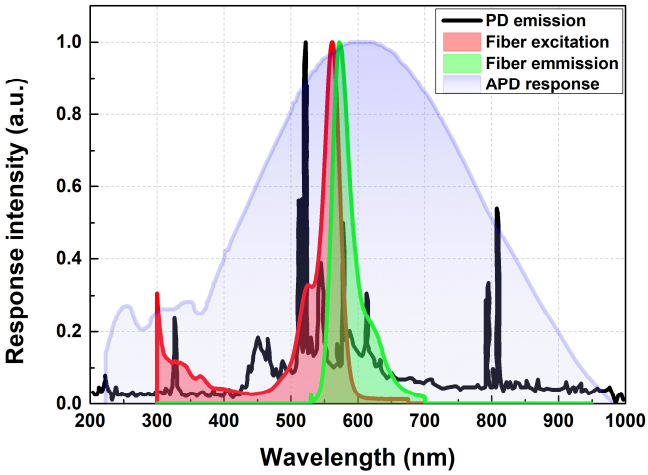

Fig. 2. The relationship of different spectral distributions.

III. Experiment Setup Design and Performance Verification

A. PCB design

The experimental PCB board structure is designed as a kind of double-curved copper track prevalent in the circuit structure (like two adjacent pins). The specific dimensional parameters and 3D perspective view of the experimental PCB are shown in Fig. 3. The PCB substrate is made of glass fiber reinforced epoxy FR4. In order to better apply the voltage, two exposed copper tracks are designed on the back side of the PCB, which are connected to the copper tracks on the front side through the through-holes of the board. The front side of the PCB is coated with the solder mask in addition to the area where the copper conductors are closest to each other, ensuring that the area where the PD occurs is not affected by the electrodes. The closest distance between copper tracks is 0.5 mm, which meets the requirement of the industrial test standard (IPC 2221-A) of a minimum distance of more than 0.25 mm. The height of the copper track is 60um.

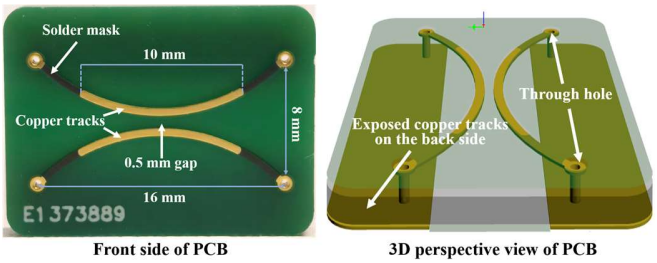

Fig. 3. Front side of PCB design (real PCB sample) and 3D perspective view of the whole PCB.

B. Conformal coating of the PCB

PCBs in MEA/AEA are subjected to harsh electrical, mechanical and environmental conditions. To improve the stability and insulation strength of the PCB, the surface of the PCB is usually coated with a protective layer to protect the PCB surface, called conformal coating. Silicone is widely used as a conformal coating in the aerospace industry due to its good performance at extreme temperatures (-50 to +125°C), excellent resistance to moisture and stable chemical properties. According to the IPC-CC-830 standard, the typical thickness of the coating is 12.5um to 200um [17]. The silicone (type: FSC 400) is used for the conformal coating material for spraying on the PCB, and the thickness is controlled to about 40um.

Before spraying the silicone, the PCB is cleaned sufficiently with isopropyl alcohol and the surface is wiped with a non-woven tissue. The fully cleaned PCB is placed horizontally in a ventilating cabinet and sprayed with silicon evenly at an inclination of 45°. Then, the sprayed PCB is smoothly placed in a drying oven for 4 hours at 60°C. The completed coated PCB is used as the final experimental sample.

C. Experiment setup and content

Fig. 4 illustrates the optical PD experimental setup for PCBs. The PCB sample is placed inside a sealed chamber to apply voltage. The test chamber can be used to change the air pressure inside by means of a vacuum pump. Sine and square wave voltages of different frequencies are applied to the PCB by using a waveform generator and a Trek 30/20A HV amplifier. The fluorescent fiber is randomly arranged around the inner cylinder of the chamber to collect the optical PD signal. The random winding arrangement of fiber is used to demonstrate that the optical detection method is still able to detect the PD signal in the presence of some blocking objects. The optical signals are collected by APD and transmitted to an oscilloscope (Picoscope 6.0). At the same time, a high-frequency current transformer (HFCT) is installed on the ground wire to detect the PD simultaneously, to compare and ensure that the PD occurred. The test chamber and sensors are placed inside a dark box, which can be regard as the pre-qualification testing of PCBs.

Regarding the operating conditions that PCBs will face in MEA/AEA, the PD phenomenon of PCBs under low air pressure and high frequency voltage is studied in the paper. Three types of air pressure conditions are conducted: 1 atmosphere (atm), 0.5 atm, and 0.1 atm, which are the atmospheric pressures at the typical cruising altitude of the aircraft. Six types of voltage conditions are applied: 50Hz AC voltage, 400Hz AC voltage, 1kHz AC voltage, 50Hz square (Squ) voltage, 1kHz square voltage and 2kHz square voltage.

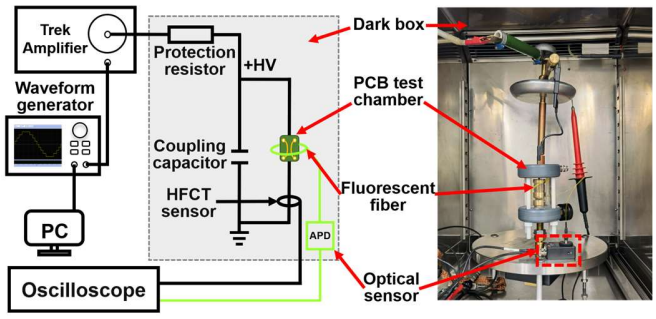

Fig. 4. Optical PD experiment platform for PCB.

In addition, to verify the reliability of the optical detection method proposed in this paper for the detection distance, the distance between the fluorescent fiber and the PCB after removing the cylinder of the chamber for the experiment is changed. Since all positions of the fluorescent fiber can receive optical signals, it is difficult to determine which region to use to calculate the distance from the PCB. Therefore, we wrapped the outer layer of the fluorescent fiber with the opaque insulating sheath, leaving only a 2 cm area for light sensing, as shown in Fig. 5. In Fig. 5, the PCB is fixed by 4 screws in the notches of two brass cylinders. The conductivity is achieved by the bare conductors on the back side of the PCB and the brass cylinders pressed against each other. The two copper tracks on the front side of the PCB are connected to the bare conductors on the back side by through holes, as shown on the right side in Fig. 3 above. The upper and lower brass cylinders apply voltage and ground respectively. The test chamber is pumped and deflated by means of the gas valve. The sensing area is placed facing the front side of the PCB and the fiber position is moved horizontally away from the PCB to achieve PD light signal acquisition at different distances.

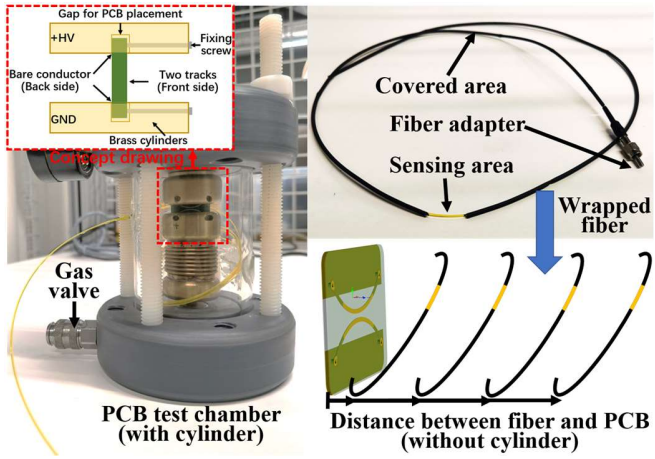

Fig. 5. Physical view of the PCB test chamber, the partially wrapped fluorescent fiber and the schematic diagram of changing the distance between the fiber and the PCB.

IV. Performance Verification of Optical Detection Method

A. Anti-interference performance

The material of the fluorescent optical fiber is polymethyl methacrylate (PMMA) and the collected signal is photonic radiation. In terms of both sensing material and signal acquisition, PMMA is a widely used plastic product, and it is completely immune to electromagnetic and acoustic signals. In addition, another advantage of using fluorescent optical fiber in this paper is that it is simple and universally applicable, so its anti-interference properties can be understood intuitively.

In the actual operation condition, there are many fast dV/dt square wave or multi-level PWM voltages in the power system of MEA/AEA, which can bring electromagnetic interference to the traditional electrical signal-based PD detection [22]. However, the optical detection-based method proposed in this paper can solve this problem well. The fluorescent optical fiber is well immune to external electromagnetic interference signals. It is proved that the fluorescent optical fiber-based detection method proposed in this paper is well suited for PD detection of PCBs in MEA/AEA. In addition, for pre-qualification of the PCBs under realistic condition, PCBs must be tested under real stress present under operation. Therefore, the optical PD detection method proposed in this paper can also provide factory acceptance test under good anti-interference condition for PCBs.

B. Verification of detection distance

The location of PD on the actual PCB is uncertain, which imposes a requirement on the PD detection method in terms of detection distance. To verify the effect of detection distance on the fluorescent fiber-based detection method, the PD is generated with the same applied voltage and the distance between the fiber and the PCB is varied to detect the PD, as shown in Fig. 6.

Since comparing only the absolute intensity of optical signals at different distances may have the effect of inherent biases such as background noise, two ways are used in this paper to express the detection effect at different distances. One is the ratio of the optical signal to the noise (OSNR), and the other is the ratio of the intensity of the electrical signal to the optical signal (EOSR), expressed as follows.

$$OSNR = mean(\sum_{i=1}^{n} 10log\frac{O_i}{B_i}) \quad (1)$$

$$EOSR = mean(\sum_{i=1}^{n} \frac{E_i}{O_i}) \quad (2)$$

where n is the number of PD pulses, O_i is the amplitude of the i-th optical PD pulse, B_i is the background noise amplitude at the i-th optical local discharge pulse, E_i is the amplitude of the i-th electrical PD pulse, *mean* represents the average value. A bigger OSNR indicates a stronger optical signal. Differently, a smaller EOSR indicates a stronger optical signal.

Limited by the size of the experimental black box, 10 distances are selected from 1cm to 40cm apart between PCB and fiber for PD detection. 500 PD pulses are collected at each position to calculate OSNR and EOSR, and the results of Fig. 6 are obtained. As can be seen in Fig. 6, the intensity of the light signal collected by the optical method gradually decreases as the distance increases. At a distance of less than about 5 cm, the intensity of the optical signal decreases very significantly. However, when the distance is more than about 5cm, with the increase of distance, the collected light signal intensity decreases at a slower rate. This is because the light is more densely distributed closer to the light source. Moreover, the sensing area of the fiber is able to cover a wider angle of direct light radiation from the PD source when the fiber is closer to the light source. As the distance of the fiber from the light source increases, the angle change of the radiated light becomes less and less obvious. Even when light radiates to infinity, the light can be considered as parallel light. When the distance reaches 40cm, the value of OSNR is still 17dB, which meets the requirement of the IEC 60270:2000 standard stating that the background noise of PD measurement should be less than 50% of the detection signal (OSNR>6dB). Although the IEC standard addresses the electrical detection signal, which is

different from the optical signal in this paper, both can reflect the magnitude of partial discharge by the magnitude of the detection value. Therefore, we use the relevant requirements of the IEC standard to compare the detection performance of the method in this paper, and obtain that the detection method in this paper meets the standard of electrical PD detection in terms of optical apparent value. Moreover, considering the high flexibility and low cost of fluorescent optical fiber, it can be arranged in a distributed manner on the PCB. The distributed arrangement can cover a wider detection range than just using a small section of fiber to sense PD. Therefore, considering the actual PCB package size in the aircraft comprehensively, a detection range of at least 40cm is fundamentally sufficient to meet the detection requirements.

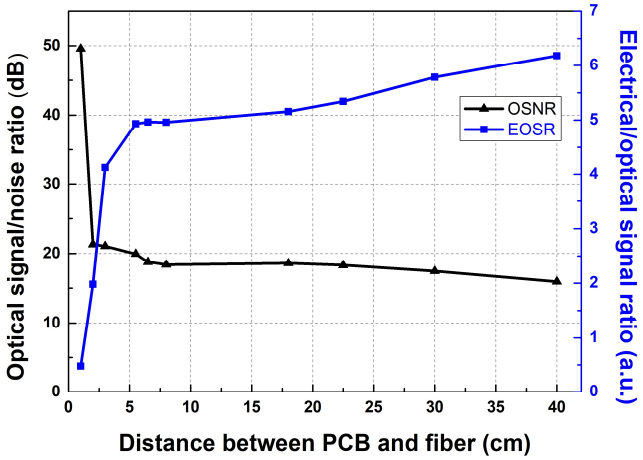

Fig. 6. The effect of distance on the optical detection method.

V. PD PHENOMENA ANALYSIS FOR PCB

A. Single PD pulse

In this paper, the electrical PD pulses collected by HFCT are compared with the optical PD pulses collected by the optical method, as shown in Fig. 7. Since the optical signal is collected with photon intensity, it has only positive polarity. While the electrical pulse has positive and negative polarity due to the different direction of the PD pulse current. The comparison reveals that the optical pulse has less oscillation near the peak, while the electrical pulse has a larger oscillation. In terms of time, the optical PD pulse is delayed by about 20 ns compared to the electrical PD pulse. This delay is due to the time required to excite the fluorescent substances after sensing the PD light in the fluorescent fiber, and the light intensity is collected as an integration of photons over a short period of time, which both produce a certain time delay. In addition, both optical and electrical pulses oscillate at the end of the pulse, but the frequencies can be found to be inconsistent.

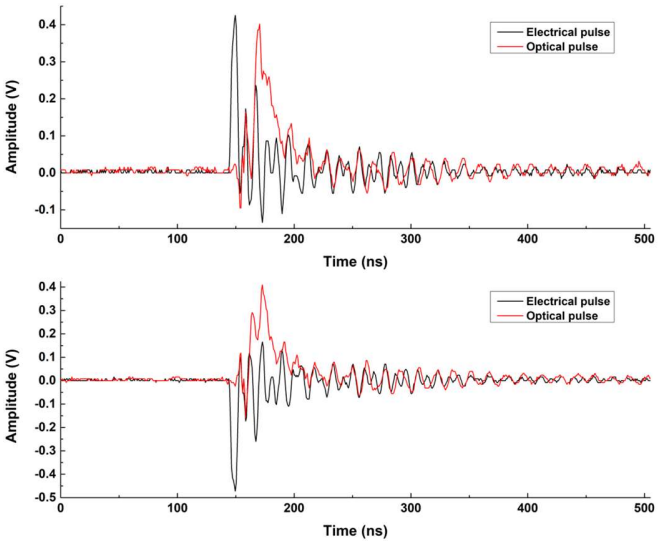

Fig. 7. The unipolar optical pulses and bipolar electrical pulses of a PD.

B. Optical PRPD pattern analysis

In order to investigate the phase distribution of PDs on PCBs at different voltage waveforms and different air pressures, 500 PD pulses are collected by the optical detection method for each experimental condition in this paper. The PRPD patterns for different experimental conditions are shown in Fig. 8.

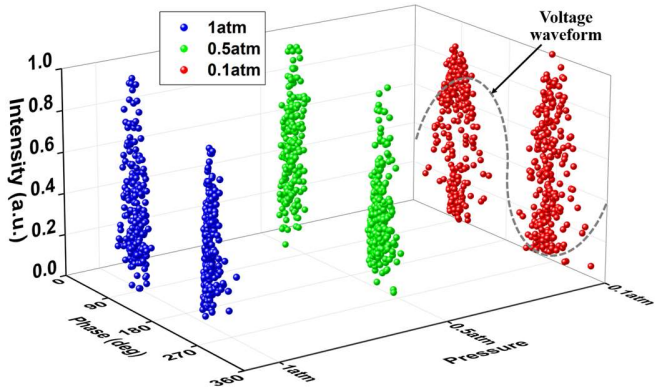

(a) PRPD pattern under AC50Hz voltage at 3 different air pressures.

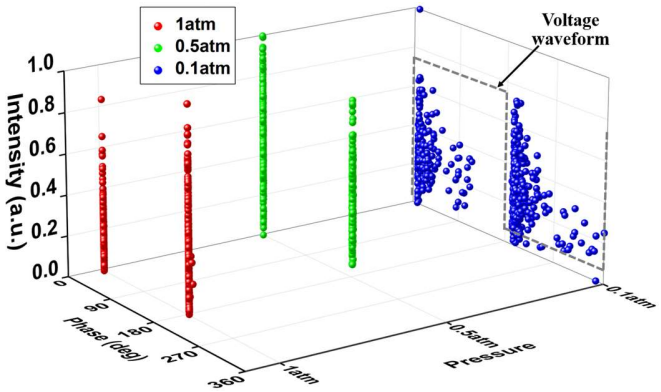

(b) PRPD pattern under Squ50Hz voltage at 3 different air pressures.

Fig. 8 Optical PRPD patterns of PCB under different conditions.

This article has been accepted for publication in IEEE Transactions on Transportation Electrification. This is the author's version which has not been fully edited and content may change prior to final publication. Citation information: DOI 10.1109/TTE.2022.3191308

Comparing the different voltages at 1 atm, it can be seen that the PDs at AC50Hz voltage are mainly distributed at the rising edge of the voltage, while the PDs at Squ50Hz voltage are mainly distributed near the voltage transition edge at 0° and 180°. This is because when the voltage rises above the inception voltage of PD (PDIV), the discharge can be generated on the PCB. However, the surface charges deposed on the PCB surface after one PD can counteract the main electric field formed by the applied voltage, forming an overall electric field (less than the PD generation condition). When the applied voltage continues to increase, the overall electric field can also gradually increase leading to the occurrence of the next PD. Therefore, the PDs at AC50Hz voltage are mainly distributed in the rising edge (absolute value), and less in the falling edge (absolute value). At the Squ50Hz voltage, the PDs are mainly distributed at the transition edge of the voltage, while the DC component of the voltage is unable to generate PDs again at the same voltage level because of the counteracting effect of the surface charge on the applied electric field. And the time needed for the surface charges to decay is much longer than the half period of the applied voltage.

However, the phase distribution of the PD gradually becomes wider as the air pressure decreases. PDs start to appear at both the falling edge of the AC50Hz voltage and the DC component of the Squ50Hz voltage, especially with the air pressure of 0.1 atm. For this phenomenon, the electric field distribution of the applied voltage PCB is simulated to understand the PD mechanism of PCB more clearly. A two-dimensional finite element simulation model of the PCB used in this paper is built in COMSOL software, which is the cross-sectional structure of the two copper tracks at the closest distance from each other. The thickness of the conformal coating in the simulation is chosen as 40μm average thickness. Then, a voltage of 4kV is applied to one copper track and the other is grounded, and the electric field distribution is obtained as shown in Fig. 9.

From the simulation result in Fig. 9, the location of the maximum field strength on the PCB is at the junction (Area 1) of the copper track, the conformal coating and the FR4 substrate. Also, there is an area of high electric field on the surface (Area 2) where the conformal coating interfaces with the air. In this case, the highest field strength in Area 1 is about four times higher than the highest field strength in Area 2. The perpendicular dielectric strength of the silicone coating used in this experiment is 80 kV/mm. Although there is an interface between the PCB and coating which has lower dielectric strength, the dielectric strength in the interface is still much higher than the dielectric strength of air at 1atm (3 kV/mm). This means that although Area 1 has a higher field strength, the PD on the PCB is more likely to occur on the surface of the coating rather than inside the coating.

By analyzing the discharge mechanism and phase distribution, we believe that the main factor affecting the differences in PRPD patterns at different air pressures is the stochastic time lag. The stochastic time lag characterizes the required time from the appearance of the first effective electron to the effective ionization, which is determined by the generation rate of the effective electron. Changing generation rate of the effective electron can influence the spatial charge distribution and the temporal development of discharges. In addition, the generation rate of the effective electron is closely related to the density of negative ions in the gas, which is dependent on the air pressure [23]. When the air pressure decreases, the density of negative ions on the interface between the air and the conformal coating decreases, which results in a lower generation rate of the effective electron and thus a longer time lag. The presence of a longer PD time lag delays the appearance of a portion of the discharge to a higher phase position, especially when the air pressure is reduced to 0.1 atm. Therefore, the phase distribution of the PRPD pattern is extended toward the region of high phase value in the positive and negative half-cycle at lower air pressure.

In addition, during the analysis of PRPD patterns, the HFCT PD signals are acquired simultaneously. It is observed that each HFCT pulse corresponds to the optical pulse one by one. Therefore, the laws obtained by the optical PRPD pattern analysis can also reflect the electrical PRPD pattern. This indicates that the optical detection method proposed in this paper can replace the traditional electrical PD detection in the PRPD pattern analysis with good application effect.

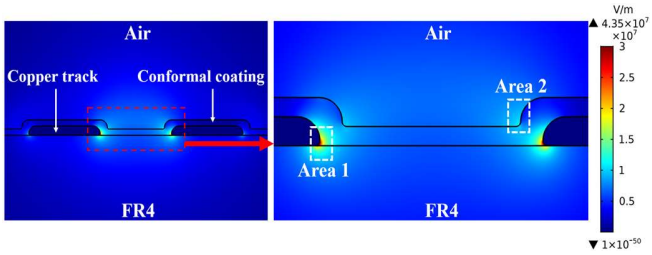

Fig. 9. Simulation of the electric field at the closest distance between the copper tracks on the PCB.

C. PD inception voltage in different conditions

PCBs in aircraft are subjected to unfavorable environments with low air pressure and high-frequency voltages, which can affect the PDIV. In this paper, experiments are conducted at three air pressures and six types of voltages (AC50Hz, AC400Hz, AC1kHz, Squ50Hz, Squ1kHz, Squ2kHz) in order to study the effects of various operating environments on the PDIV. In addition, both optical and HFCT detection methods are used in the experiments to compare the detection sensitivity of the optical method in various environments.

In the experiments, it is found that the PD on PCBs have episodic and unstable discharges. Therefore, when the PD pulses appear continuously and steadily, the voltage at this time is recorded as PDIV in this paper. The experimental results show that the PDIV recorded by both methods is the same, which indicates that the optical detection method and the electrical detection method have the same sensitivity in detecting the PDIV. The PDIV under various operating conditions are shown in Fig. 10. When the PD pulse occurs uninterruptedly within 20 s, the voltage at this time is defined as PDIV in this paper. In the experimental, five PCB samples are selected for experiments under each condition. Because the coating thickness of the PCB surface is difficult to accurately control the exact same by spraying, so even under the exact same experimental conditions PDIV will be affected by the difference in thickness. Therefore, the value of PDIV in this paper is chosen as the median value of the 5 sets of data.

From Fig. 10, it is obtained that PDIV decreases with decreasing air pressure for all types of voltages, which is also consistent with the description of the relationship between PD and air pressure in the previous section. When the air pressure decreases from 1 atm to 0.5 atm, the PDIV decreases significantly for all voltage types. However, when the air pressure decreases from 0.5 atm to 0.1 atm, there is only a small decrease in PDIV under all voltage types. This indicates that when the air pressure is reduced to a very low level, although the average free path $\bar{\lambda}$ of electrons is large, the reduction of gas molecules also reduces the possibility of electron avalanche generation at the same time, which is in accordance with the theory of the Paschen's curve.

For the voltages of the same waveform in Fig. 10, the PDIV decreases with increasing frequency, which is related to the space charge and dielectric loss on the surface of the PCB coating. When a smaller avalanche that is difficult to be detected is generated at one polarity of the alternating electric field, it can induce space charges with the opposite distribution of the electric field polarity at this time, which will weaken the whole electric field strength on the surface of the PCB. These space charges can dissipate in a certain period of time. However, if the space charges are not completely dissipated during the application time of the alternating electric field of the same polarity, when the polarity of the alternating electric field becomes opposite, these space charges will instead enhance the overall electric field strength on the surface of the PCB. Therefore, when the frequency of the alternating voltage is higher, the space charge dissipates for a shorter time under the voltage of the same polarity. The residual space charge that does not dissipate will make the overall electric field strength under the next opposite polarity field stronger, and thus more likely to generate PD. The schematic diagram of the change process of space charges at a higher voltage frequency is shown in Fig. 11.

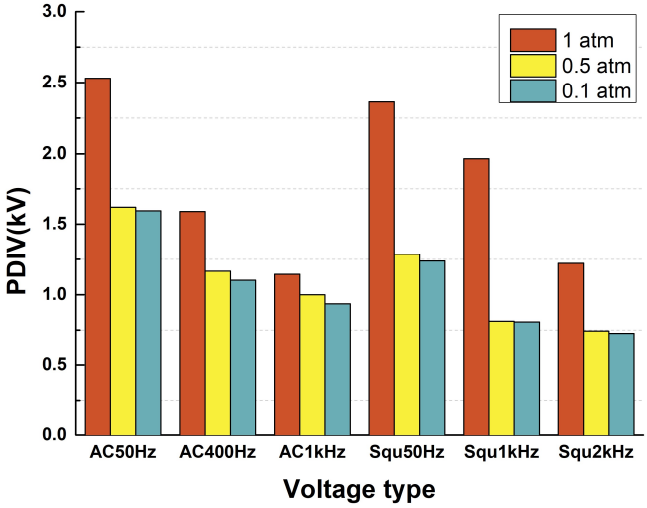

Fig. 10. PDIV under various operating conditions.

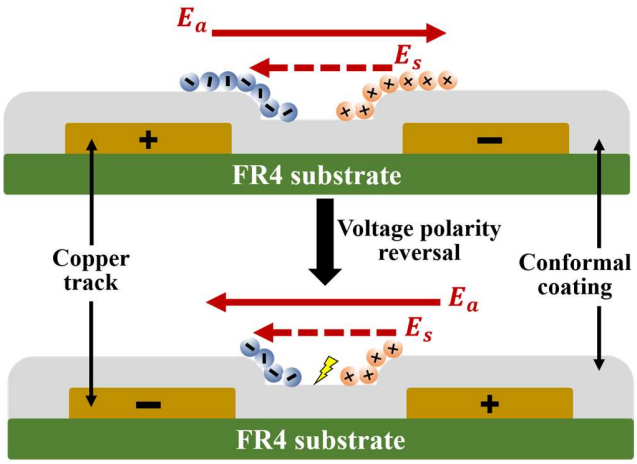

Fig. 11. Changes in the distribution of space charges and electric field on the PCB surface before and after the voltage polarity reversal. The space charge cannot be dissipated all within the same voltage polarity because of the high voltage frequency.

In addition, the dielectric loss of the insulation material is also affected by the voltage frequency. According to the principle of dielectric loss of solid insulation, the relationship between dielectric loss and frequency can be expressed as follows.

$$\varepsilon''_{r,app} = \varepsilon''_r + \frac{\sigma}{\omega\varepsilon_0} \tag{3}$$

$$\frac{dP}{dv} = \omega\varepsilon_0\varepsilon''_{r,app}|\boldsymbol{E}|^2 \tag{4}$$

where $\varepsilon''_{r,app}$ is the apparent relative permittivity, ε''_r is the imaginary part of complex relative permittivity, ω is the angular frequency, σ is the conductivity, P is the dielectric loss, $\boldsymbol{E}$ is the electric field [24].

From (3) and (4), it can be seen that the dielectric loss increases with the increase of voltage frequency when the electric field strength is constant. At the same time, due to the influence of the space charges, the overall electric field strength of the PCB surface will also be enhanced with the rise in voltage frequency (as mentioned in the previous), which can also increase the dielectric loss of the insulation. The increase in dielectric loss can lead to local heating in the insulation at the microscopic level, which will exacerbate the PD generation. Therefore, as the voltage frequency increases, the PDIV of the PCB gradually decreases.

What's more, for the voltages of the same waveform, the decrease of PDIV in 1atm is bigger than the decrease in the remaining two low air pressures. Moreover, the difference between the PDIV in 1atm and the PDIV in the other two low air pressures decreases as the frequency increases. This indicates that when the frequency of voltage increases to a certain level, the influence of air pressure on PDIV will no longer dominate. This means that the high-frequency voltage used in the semiconductor switching devices that are currently widely used in aircraft has a greater impact on the PCB, which should be given attention.

This article has been accepted for publication in IEEE Transactions on Transportation Electrification. This is the author's version which has not been fully edited and content may change prior to final publication. Citation information: DOI 10.1109/TTE.2022.3191308

VI. Relationship Between Optical Signal and PD Magnitude

In order to obtain the relationship between the PD light signal and the PD current amplitude (apparent discharge) of the PCB under different operating conditions, PD experiments at different air pressures and different voltages are conducted in this paper. The experiments are divided into two parts for analysis. The first part is the relationship between the optical signal and the PD amplitude at different air pressures when the voltage is kept constant. The second part is the relationship between the light signal and the PD amplitude at different voltages when the air pressure is kept constant (typical air pressure in aircraft is 0.5 atm [5]). Two kinds of signals are collected simultaneously for each experimental condition, and then the relationship between the two signal intensities is studied. Since there are negative polarity PD pulses in the electrical signals, the positive and negative polarities are shown separately.

The relationship between the optical PD signal and the PD amplitude of the PCB in different conditions are shown in Fig. 12 and Fig. 13. As shown in Fig. 12 and Fig. 13, there are some trend differences between positive and negative polarity discharges in relation to the optical signal amplitude, which is probably caused by microscopic differences between the two electrodes.

For the experimental case with a certain voltage but different air pressure, two typical voltage types of PCB PDs are studied, namely AC50Hz and Squ50Hz. It can be seen that the absolute value of PD amplitude is proportional to the optical signal amplitude under any air pressure. When the PD amplitude is small, the trend of increasing optical signal amplitude with increasing PD amplitude is flatter, and this phenomenon is more apparent at Squ50Hz voltage. This relationship becomes more obvious as the PD amplitude increases. Fig. 12 illustrates that the detection method proposed in this paper can effectively respond to the PD magnitude at all air pressures.

For different voltages with the same air pressure, the relationship between the absolute value of the PD amplitude and the optical signal amplitude also remains positively proportional in the case of voltage frequency change. Moreover, the proportional relationship between the two signals becomes more evident as the voltage frequency increases.

Overall, there is a clear proportional relationship between the optical PD signal and the PD amplitude. This indicates that the PD severity on PCBs can be effectively assessed by the optical detection method proposed in this paper. It is of good application value to determine the potential fault risk on PCB by detecting the intensity of optical PD signals.

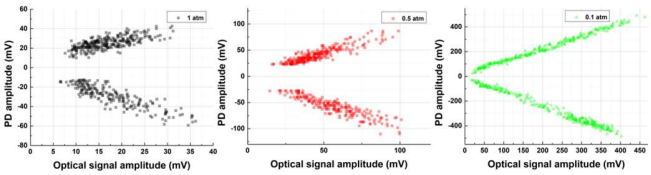

(a) PCB under the AC50Hz voltage for different air pressures.

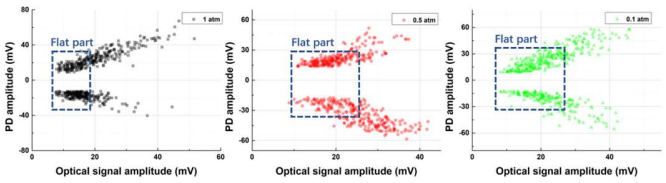

(b) PCB under the Squ50Hz voltage for different air pressures.

Fig. 12. Relationship between optical PD signal and PD amplitude under 2 kinds of voltages at different air pressures.

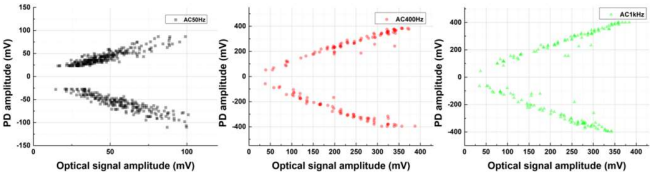

(a) PCB under AC voltage for 0.5 atm.

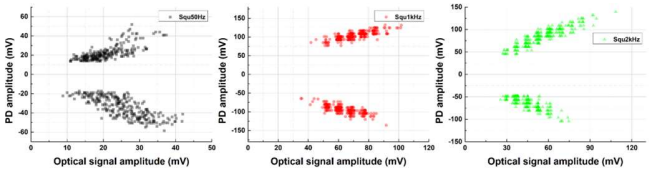

(b) PCB under Squ voltage for 0.5 atm.

Fig. 13. Relationship between optical PD signal and PD amplitude under different kinds of voltages for 0.5 atm.

VII. Conclusions

In this paper, an optical detection method that can be applied to PD detection on PCBs in electrified aircraft is proposed, and its effectiveness is demonstrated. The PD pulse signal, PRPD patterns and PDIV under different air pressure and different kinds of voltage conditions are analyzed by designing and building a PD experimental platform for PCBs based on the fluorescent fiber. Finally, the relationship between optical signal and PD amplitude is obtained. The specific conclusions are as follows.

(1) The proposed optical PD detection method based on fluorescent fiber has good immunity to electromagnetic interference and vibration interference, which can be well suited to the working environment of aircraft. Moreover, the detection range of the method can reach more than 40cm. Combined with the advantage of the distributed arrangement of optical fiber, the detection capability can fully over the space of PCB package in the electrified aircraft, which is of high practical value.

(2) The optical PD pulses on the PCB correspond to the electrical PD pulses one-to-one, proving that the optical detection method can accurately and effectively detect PDs. However, there are differences in the shape of optical and electrical PD pulses. For the PD phase distribution, the optical PRPD pattern for the PCB is mainly distributed along the rising edge of the voltage, but the distribution range expands as the air pressure decreases. In addition, the area with the highest electrical field strength is located at the junction of the copper track, FR4 substrate and conformal coating. The high frequency

and low air pressure working conditions makes it more likely that PD on the PCB occur, which is more harmful to the PCB.

(3) There is a proportional relationship between the optical signal and the PD amplitude for different air pressures and different voltage types. The magnitude of the optical signal can well reflect the PD severity, so that the insulation status of the PCB in electrified aircraft can be effectively evaluated through the optical detection method.

REFERENCE

[1] V. Madonna, P. Giangrande and M. Galea, "Electrical Power Generation in Aircraft: Review, Challenges, and Opportunities," IEEE Trans. Transp. Electrif., vol. 4, no. 3, pp. 646-659, Sept. 2018.

[2] S. W. Jee, "The Effect of Guard on Improving the Resistance to Tracking Phenomenon for the PCB," J. Electr. Eng. Technol., vol. 17, pp. 485-494, 2021.

[3] M. Borghei, M. Ghassemi, "Classification of Partial Discharge in Electric Aircraft based on Short-Term Behavior of Insulation Systems," AIAA Propulsion and Energy 2021 Forum, pp. 3294, 2021.

[4] M. Borghei and M. Ghassemi, "Insulation Materials and Systems for More- and All-Electric Aircraft: A Review Identifying Challenges and Future Research Needs," IEEE Trans. Transp. Electrif., vol. 7, no. 3, pp. 1930-1953, Sept. 2021.

[5] H. Schefer, L. Fauth, T. H. Kopp, R. Mallwitz, J. Friebe and M. Kurrat, "Discussion on Electric Power Supply Systems for All Electric Aircraft," IEEE Access, vol. 8, pp. 84188-84216, 2020.

[6] Y. Zang *et al.*, "A Novel Optical Localization Method for Partial Discharge Source Using ANFIS Virtual Sensors and Simulation Fingerprint in GIL," IEEE Trans. Instrum. Meas., vol. 70, pp. 1-11, 2021.

[7] A. Cavallini, L. Versari and L. Fornasari, "Feasibility of partial discharge detection in inverter-fed actuators used in aircrafts," 2013 Annual Report Conference on Electrical Insulation and Dielectric Phenomena, 2013, pp. 1250-1253.

[8] C. Abadie, T. Billard, S. Dinculescu and T. Lebey, "On-line non intrusive PDs' measurements on aeronautical systems," 2017 International Symposium on Electrical Insulating Materials (ISEIM), 2017, pp. 99-103.

[9] Y. Wang *et al.*, "Partial Discharge Investigation of Form-Wound Electric Machine Winding for Electric Aircraft Propulsion," IEEE Trans. Transp. Electrif., vol. 7, no. 1, pp. 78-90, March 2021.

[10] J. Jiang *et al.*, "Optical Sensing of Partial Discharge in More Electric Aircraft," IEEE Sens. J., vol. 20, no. 21, pp. 12723-12731, 1 Nov.1, 2020.

[11] M. M. Yaacob, *et al*., "Review on partial discharge detection techniques related to high voltage power equipment using different sensors," Photonic Sens., vol. 4, pp. 325-337, 2014.

[12] H. Y. Zhou, et al., "Optical sensing in condition monitoring of gas insulated apparatus: a review," High Volt., vol. 4, no. 4, pp. 259-270, 2019.

[13] C. Emersic, R. Lowndes, I. Cotton, S. Rowland and R. Freer, "Observations of breakdown through printed circuit board polymer coatings via a surface pollution layer," IEEE Trans. Dielectr. Electr. Insul., vol. 24, no. 4, pp. 2570-2578, 2017.

[14] C. Emersic, R. Lowndes, I. Cotton, S. Rowland and R. Freer, "Degradation of conformal coatings on printed circuit boards due to partial discharge," IEEE Trans. Dielectr. Electr. Insul., vol. 23, no. 4, pp. 2232-2240, August 2016.

[15] H. Koch, W. Pfeiffer, H. Reinhard and H. Safran, "Partial discharge. VI: PD testing of printed circuit boards," IEEE Electr. Insul. Mag., vol. 7, no. 3, pp. 9-15, May-June 1991.

[16] I. Mantis, F. Li, M. S. Jellesen, *et al.*, "Effect of intrinsic PCB parameters on the performance of fluoropolymer coating under condensing humidity conditions," Microelectron. Reliab., vol. 122, no. 114158, 2021.

[17] E. Zeynali, R. Bridges and B. Kordi, "Electrical Insulation of Conformally Coated Printed Circuit Boards: An Overview and a Study of the Influence of Pollution," IEEE Electr. Insul. Mag., vol. 37, no. 2, pp. 6-17, March-April 2021.

[18] D. McCarthy *et al.*, "Radiation Dosimeter Using an Extrinsic Fiber Optic Sensor," IEEE Sens. J., vol. 14, no. 3, pp. 673-685, March 2014.

[19] J. H. Watterson, P. A. E. Piunno, C. C. Wust, *et al.*, "Controlling the density of nucleic acid oligomers on fiber optic sensors for enhancement of selectivity and sensitivity," Sens. Actuator B-Chem., vol. 74, no. 1-3, pp. 27-36, 2001.

[20] S. Kumari, "Feasibility Study for Usage of Optical Partial Discharge Detection in HV Cable Termination," M.S. thesis, Delft Univ. of Tech., Delft, Netherlands, 2018.

[21] J. Jiang, M. Zhao, Z. Wen, *et al.*, "Detection of DC series arc in more electric aircraft power system based on optical spectrometry," High Volt., vol. 5, no. 1, pp. 24-29, 2020.

[22] Y. Wang, *et al.* "Partial Discharge Testing Platform for High Voltage Power Module Packaging Under Square Wave Excitation," 2021 IEEE Applied Power Electronics Conference and Exposition (APEC) IEEE, 2021.

[23] P. Fu, *et al.* "The role of time-lag in the surface discharge inception under positive repetitive pulse voltage," Phys. Plasmas, vol. 25, no. 9, pp. 093518, 2018.

[24] M.G. Niasar, R.C. Kiiza, N. Taylor and H. Edin, "Effect of partial discharges on thermal breakdown of oil-impregnated paper," IEEJ Trans. Elec. Electron. Eng., vol. 10, no. S1, pp.S14-S18, 2015.